Seventh International Conference on Computational Fluid Dynamics (ICCFD7), Big Island, Hawaii, July 9-13, 2012

ICCFD7-3706

SPH Simulation of Gas Arc Welding Process

M. Ito*, S. Izawa*, Y. Fukunishi*, and M. Shigeta*
Corresponding author: masumi@fluid.mech.tohoku.ac.jp

* Tohoku University, Japan.

Abstract: TIG welding process is simulated by an SPH method, where the phase change of the anode material, the free surface movement of the liquid, and the four dominant flow-driving forces are taken into account. The effect of welding arc is given by the thermal boundary condition at the surface of the anode material. Reasonable computational results are obtained, and it is shown that the SPH method is applicable to this kind of phenomena.

Keywords: SPH, TIG welding, Arc weld pool, Surface tension, Meshless method, Multi-phase flow.

1 Introduction

Arc welding which includes TIG (Tungsten Inert Gas) welding is one of the essential technologies that supports the heavy industries. However, its technical development is largely based on the empirical knowledge and the senses of the engineers in the field, mainly because of the difficulties in the experimental measurements. Thus, the phenomena included in the arc welding are still poorly understood with many unanswered questions even on its basics, especially for a flow inside the molten metal puddle, namely the weld pool. The lack of knowledge makes an accurate prediction of the state and geometry of the arc weld pool impossible, which is needed in order to control the quality of welding.

Although computational simulation is a promising tool to investigate such a weld pool formation, because the growth of weld pool depends on various factors, surface tension and deformations of gas-liquid and solid-liquid interfaces [1], the molten pool simulations is not easy. Solving such a flow field by conventional grid-based methods is an exhaustive task since a special effort such as a regeneration of the grid is required [2]. Thus, either the high-end technical application of a grid base method or a new and undeveloped grid less method is demanded for a welding simulation.

The present paper uses an SPH (Smoothed Particle Hydrodynamics) method. SPH is a Lagrangian particle method, which is very often suitable for these problems. We have already applied SPH to molten pool convection simulations of TIG welding, and successfully simulated the generation process of a weld-pool development when the heat source is not moving [3]. The temperature and velocity distribution of a shielding gas flow are taken into account as the boundary condition so that the gas flow can be omitted from the computation process. In this study, the simulation of TIG welding is attempted under a more practical condition: The heat source on the anode surface moves at a constant speed along the joint surface of two materials.

2 Numerical Method

Lagrangian SPH method is described by the quadrature formulas on moving particles of constant mass. The quantities at the centers of the particles are obtained by summations using a kernel function $W(\boldsymbol{r}, h)$ or its derivative ∇W. The parameter h denotes the kernel smoothing radius. For example, the density at the center of a particle is approximated by summation of particles' mass distributed around them. In the present simulation, each particle moves according to its velocity, and then, the particle locations are adjusted every

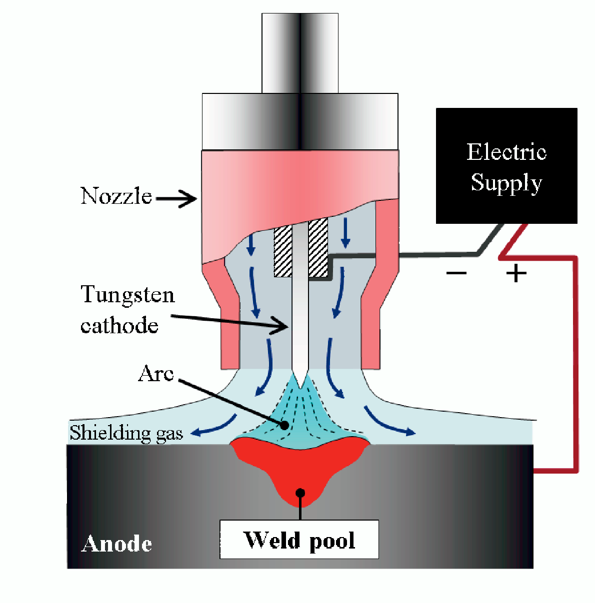

Figure 1: TIG welding system.

time step to keep the density field uniform. After that, the external forces are taken into account as follows,

$$\boldsymbol{v}_a(t+\Delta t) = \boldsymbol{v}_a(t) + \frac{\sum_n \Delta \boldsymbol{r}_a^{\mathrm{adjust},n}}{\Delta t} + \left(\frac{\boldsymbol{F}_a}{\rho_a}\right)\Delta t, \tag{1}$$

where $\Delta \boldsymbol{r}_a^{\mathrm{adjust}}$ is the displacement of particle a during the density-adjustment process. The external force $\boldsymbol{F}$ contains the viscosity, gravity and four driving forces; buoyancy, Lorentz force, friction with the shielding gas flow, and the surface tension. The detailed procedure can be found in Ref. [4].

Figure 1 depicts a schematic view of a TIG welding system. In the present computation, only the change that takes place to the anode material is simulated and its surface is heated using the temperature distribution of the shielding gas flow. In addition, the shielding gas velocity and the electric current distribution inside the anode are given as boundary conditions. The data used were provided by the courtesy of Prof. M. Tanaka, Osaka University [5].

The effect of the surface tension is resolved into the normal and tangential forces. The surface normal force is given as an attractive force of particles $\boldsymbol{F}^{\mathrm{attract}}$. When an attraction between particles is given for a particle system, the simulation often becomes unstable. Following weighted function is introduced to prevent this instability.

$$f_{ab}^{\mathrm{attract}} = f^{\mathrm{attract}}(|\boldsymbol{r}_a - \boldsymbol{r}_b|, h) = \begin{cases} q & (0 \le q < 1) \\ 2-q & (1 \le q < 2) \\ 0 & (2 \le q), \end{cases} \tag{2}$$

where $q = |\boldsymbol{r}_a - \boldsymbol{r}_b|/h$ is the non-dimensionalized distance between the particles. Using this function, the force of the surface tension is given as,

$$\boldsymbol{F}_a^{\mathrm{attract}} = d \sum_b \gamma' f_{ab}^{\mathrm{attract}}, \tag{3}$$

where d is the particle diameter, and γ' is a product of an arbitrary constant and the surface tension coefficient γ. The value of γ' is adjusted based on the results of the preliminary computation of a liquid drop oscillation.

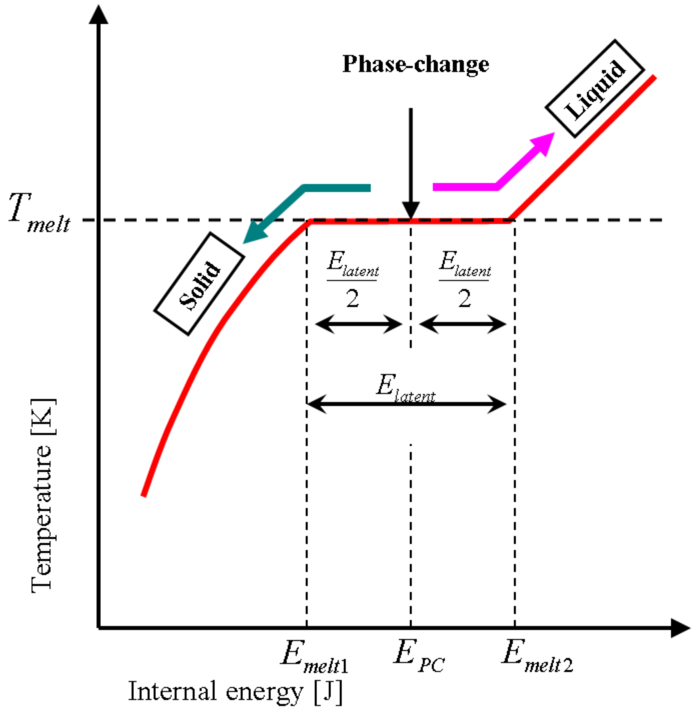

Figure 2: Handling of latent heat.

The tangential force deriving from the gradient of the surface tension is obtained from the gradient of γ with respect to T and the temperature gradient at the surface,

$$\boldsymbol{F}^{\text{tangent}} = \frac{\mathrm{d}\gamma}{\mathrm{d}T} d \cdot \boldsymbol{n} \times \nabla T \times \boldsymbol{n}, \tag{4}$$

where, $\boldsymbol{n}$ is the surface normal vector and the $\mathrm{d}\gamma/\mathrm{d}T$ is a constant with a value of 0.21 mN/mK.

Heat transfer and heat generation are written as follows:

$$\frac{\partial T_a}{\partial t} = \frac{1}{\rho_a C_a} \left\{ \frac{6}{\lambda_a} \sum_b \kappa_b (T_b - T_a) W_{ab} + Q_a \right\}, \tag{5}$$

$$\lambda_a = \sum_b (\boldsymbol{r}_b - \boldsymbol{r}_a)^2 W_{ab}, \tag{6}$$

where C is the specific heat, T is the temperature, and κ is the thermal conductivity. This is the same as the Laplacian model which is normally used in another particle method, MPS method [6]. The first term of the right hand side is the heat conduction term. The heat generation Q contains the heat generated by electrons entering the anode surface and the radiation heat loss.

The latent heat for solid-liquid phase change is taken into account. Figure 2 shows how the temperature changes with energy during the phase changes. E^{latent} is the latent heat of a particle. Here, the energy amount $E^{\text{PC}} = (E^{\text{melt1}} + E^{\text{melt2}})/2$ is defined as the energy point where a solid-liquid transition occurs.

The target is a couple of anode metal plates, SUS304 bar with 10 mm $\times$ 10 mm cross section and 100 mm length, placed 1 mm away from each other

They are heated in a manner as in a TIG welding. The effect the gap will have on the magnetic and electric fields are neglected.

The heat source position x_c and y_c are changed as follows:

$$x_c = 0.0, y_c = \begin{cases} 1.0 & (0.0 \leq t < 1.0) \\ 1.0 + 5.0t & (1.0 \leq t). \end{cases} \quad (7)$$

The moving velocity of heat source is adjusted based on the results of preliminary simulations, so that the penetration depth will reach around a half of the anode height.

3 Results and discussion

Figure 3 shows the overview of the welding process. The colors indicate a phase or a temperature of the particles. Gray indicates a solid state and magenta indicates the melting point. The white cathode bar drawn in the figures merely indicates the heater position. It is found that the high-temperature regions melt, fuse, and consequently form a liquid puddle. The molten metal penetrates into the clearance between the two metals and it soon becomes solidified. Since the heating position is fixed until $t \leq 1.0$ s, the high-temperature region initially forms a circle. When heating position starts to move along the weld line, the shape of weld pool becomes elongated, and is solidified at the end. Once the heat source reaches the other end, the molten metal drops from the plate, as shown in the figure.

Figure 3 shows the time evolution of the temperature distribution in a cross section at the median center between both anode ends. The gap between two anodes are buried by the molten metal at around t=9.0 s. After the heat source passes, the melted metal is solidified and the two plates become welded together.

4 Conclusion

SPH simulation of TIG welding process was carried out. Two anode material plates were placed with a gap and then melted and fused by the heat of a TIG welding process. The heat source was moved at a constant speed. As a result, the behavior of the molten material as fluid and the progress of the weld penetration could be simulated. After the heat source passed away, the molten material solidified as the temperature decreased.

These results show the potential and usefulness of the SPH method in phase changing problems as in the welding simulation.

References

[1] P. S. Wei. Thermal Science of Weld Bead Defects: A Review. *J. Heat Transfer*, 133(3):31005, 2011.

[2] G. R. Liu and M. B. Liu. *Smoothed Particle Hydrodynamics: A Meshfree Particle Method.* World Scientific Pub. Co. Inc., 2003.

[3] M. Shigeta, M. Ito, S. Izawa, and Y. Fukunishi. Three-dimensional simulation of a flow in an arc weld pool by SPH method. *Proceedings of The International Symposium on Visualization in Joining & Welding Science through Advanced Measurements and Simulation*, 1:9–10, 2010. Osaka, Japan, November 11-12.

[4] M. Shigeta, T. Watanabe, S. Izawa, and Y. Fukunishi. Incompressible SPH Simulation of Double-Diffusive Convection Phenomena. *International Journal of Emerging Multidisciplinary Fluid Sciences*, 1(1):1–18, 2009.

[5] M. Tanaka, H. Terasaki, M. Ushio, and J. J. Lowke. Numerical Study of a Free-burning Argon Arc with Anode Melting. *Plasma Chemistry and Plasma Processing*, 23(3):585–606, 2003.

[6] S. Koshizuka and Y. Oka. Moving-particle Semi-implicit Method for Fragmentation of Incompressible Fluid. *Nucl. Sci. Eng.*, 123:421–434, 1996.

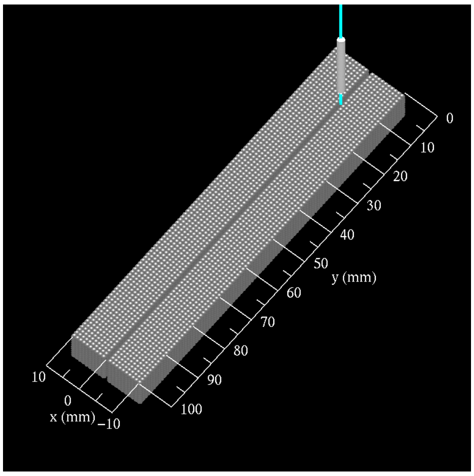

t=0.0 s

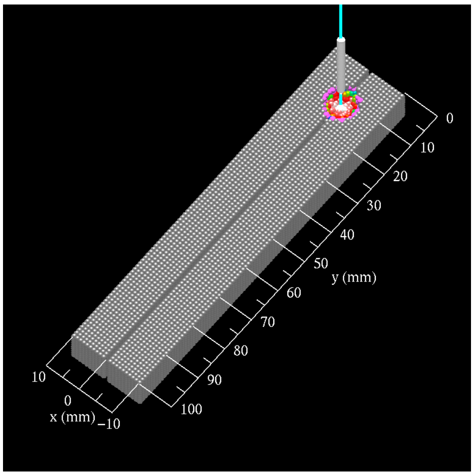

t=1.0 s

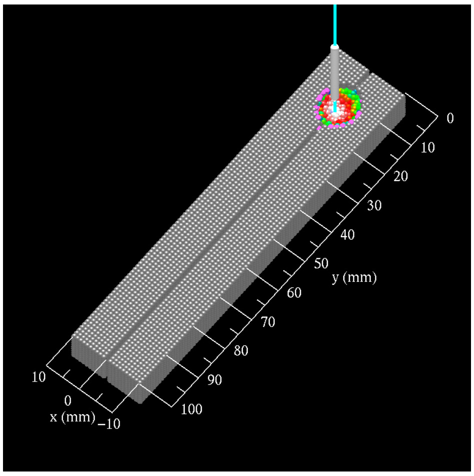

t=2.0 s

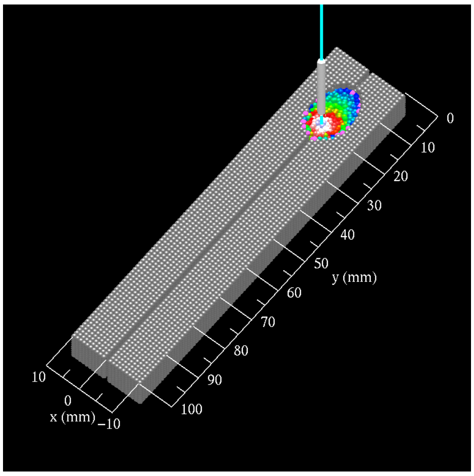

t=3.0 s

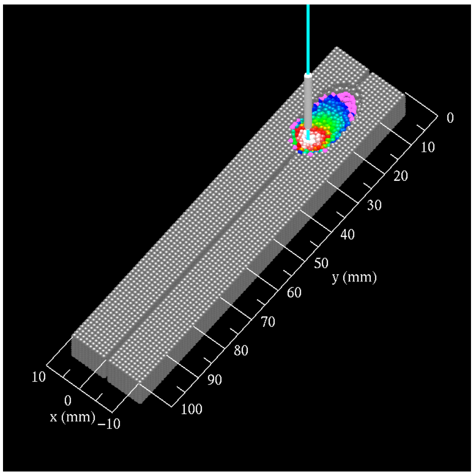

t=4.0 s

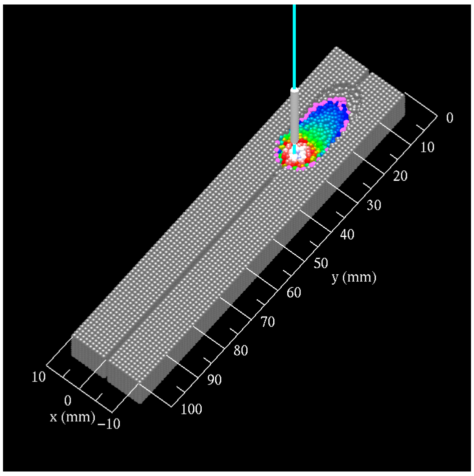

t=5.0 s

Figure 3: Time evolution of SUS304 bars heated by TIG welding heat source.

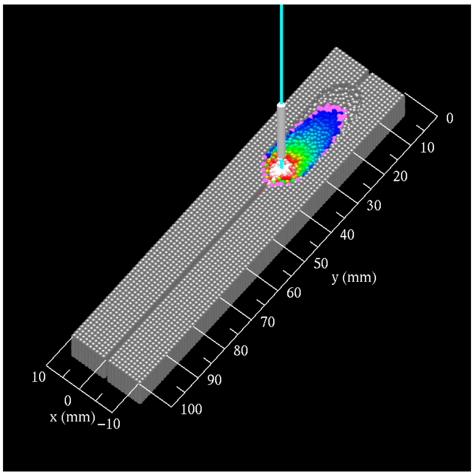

t=6.0 s

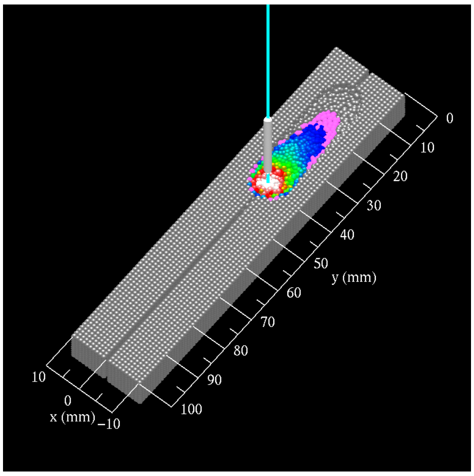

t=7.0 s

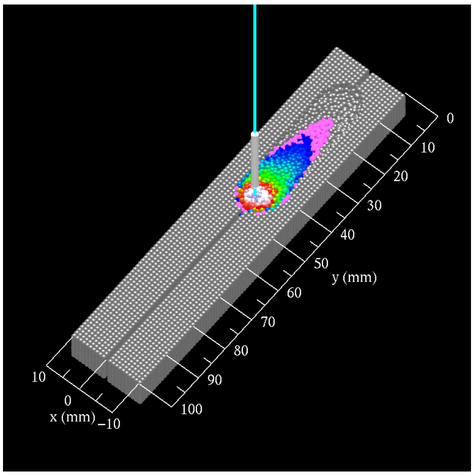

t=8.0 s

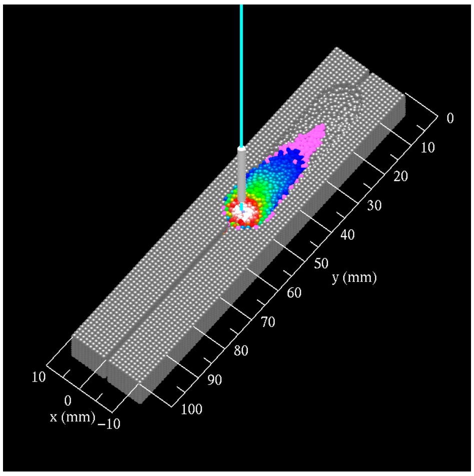

t=9.0 s

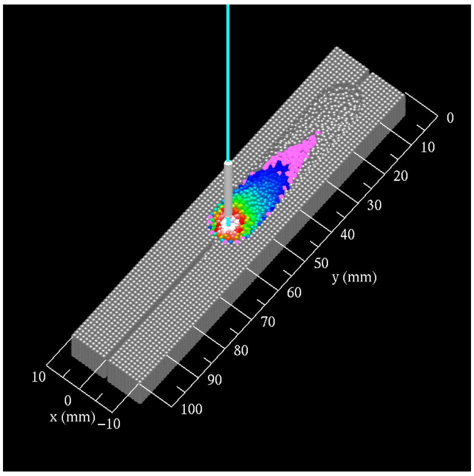

t=10.0 s

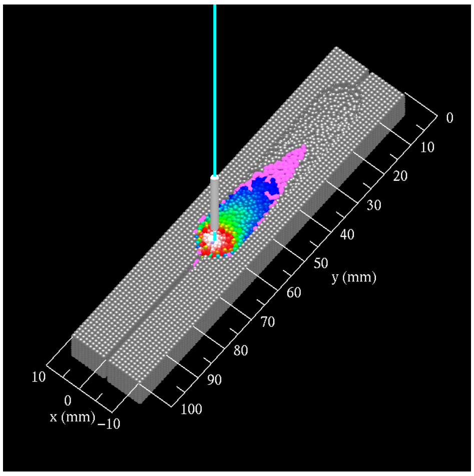

t=11.0 s

Figure 3 continued.

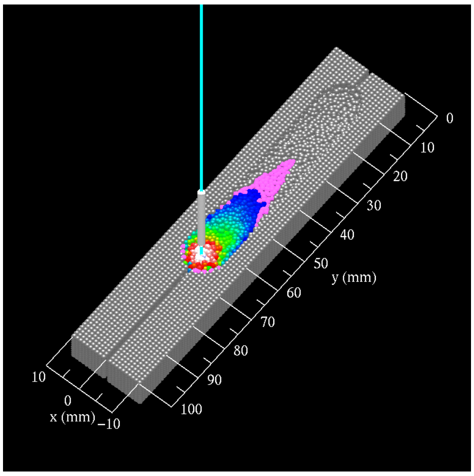

t=12.0 s

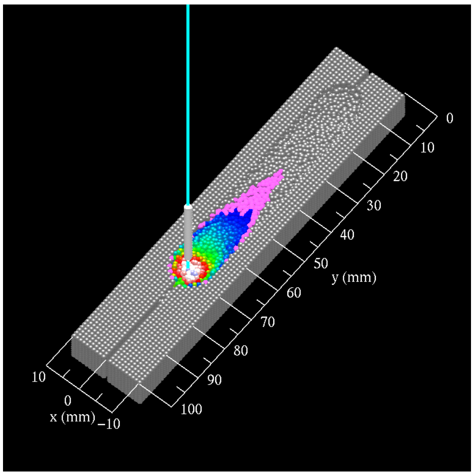

t=13.0 s

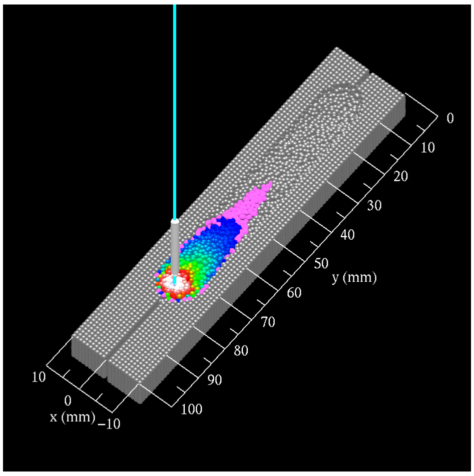

t=14.0 s

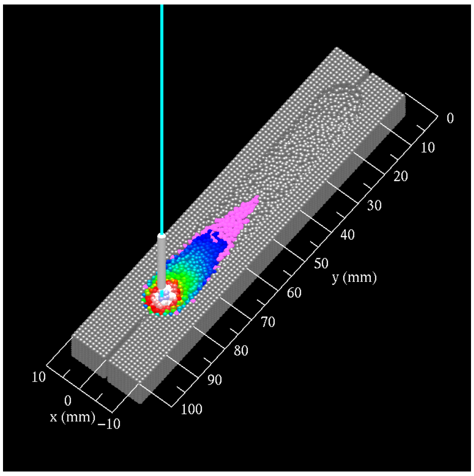

t=15.0 s

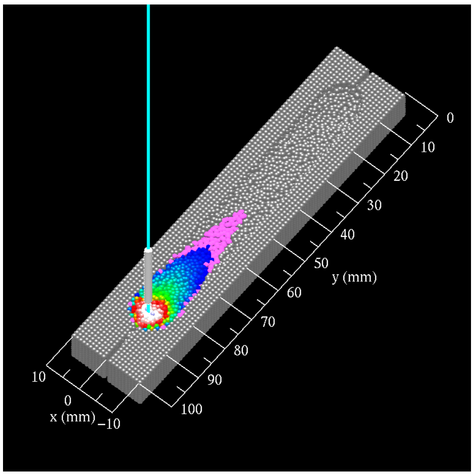

t=16.0 s

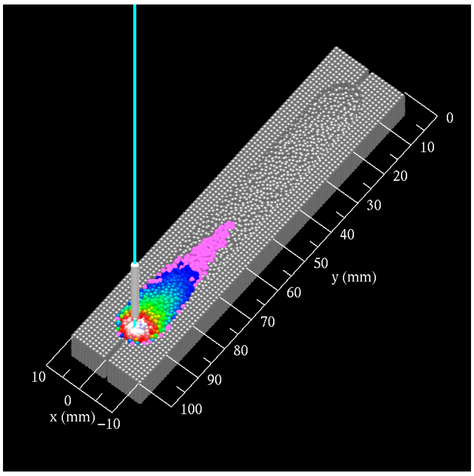

t=17.0 s

Figure 3 continued.

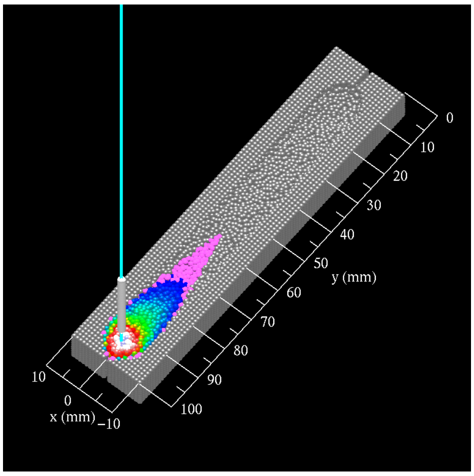

t=18.0 s

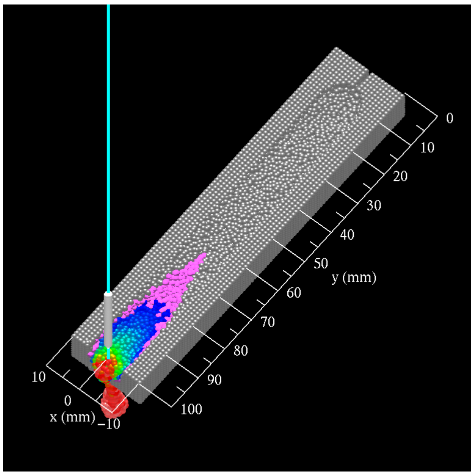

t=19.0 s

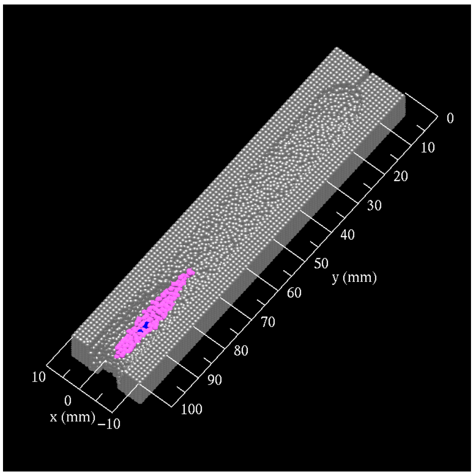

t=20.0 s

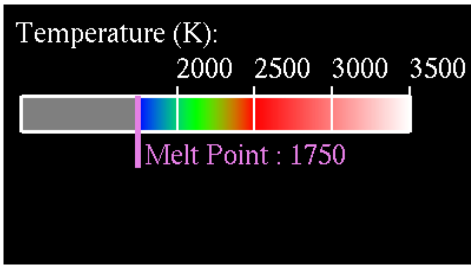

legend

Figure 3 continued.

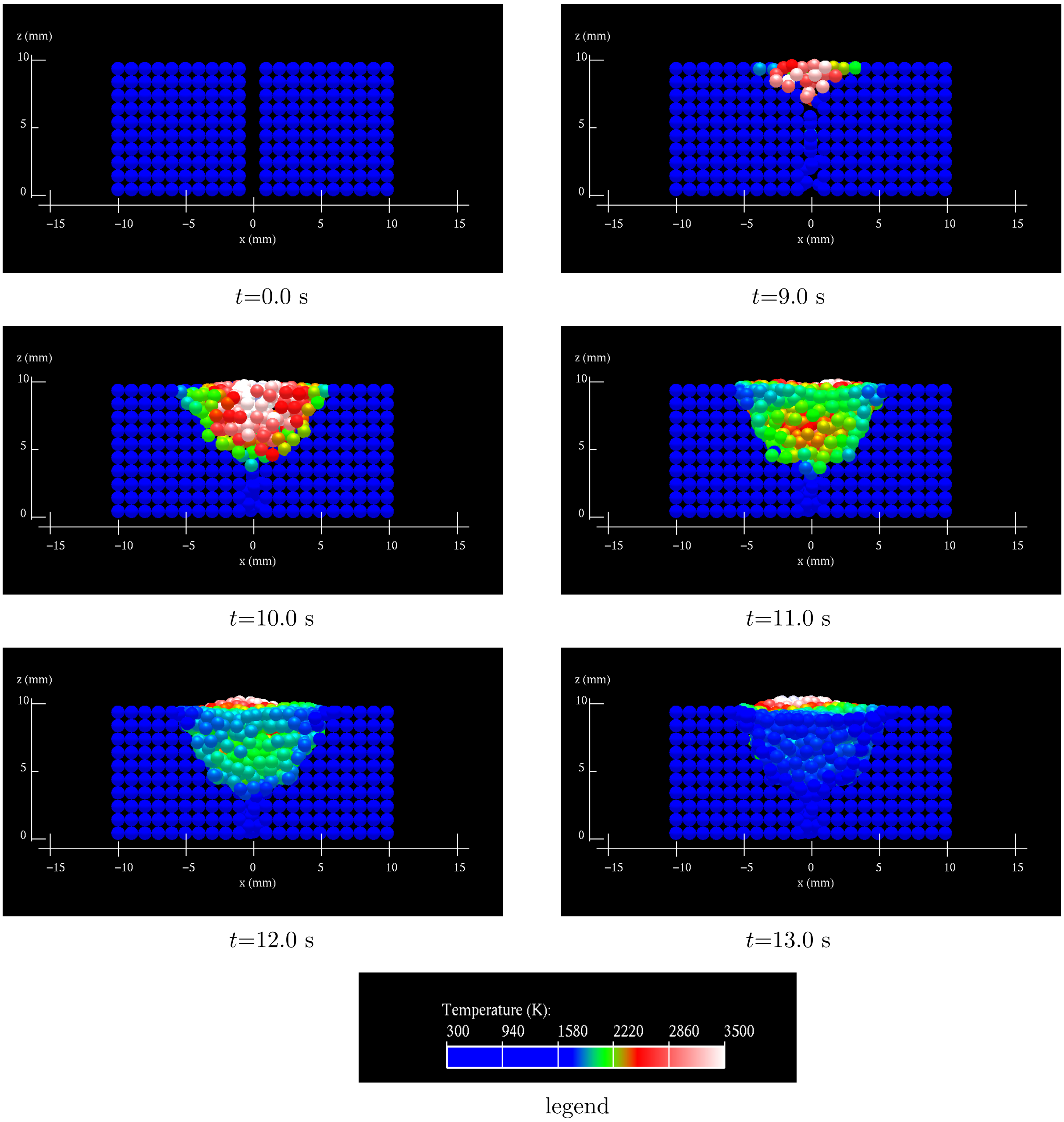

Figure 4: Time evolution of temperature distribution in cross section including median center.